JOURNAL OF MATERIALS SCIENCE 26 (1991) 307–320

Residual strength and toughness of damaged composites

B. HARRIS, A. S. CHEN, S. L. COLEMAN, R. J. MOORE
School of Materials Science, University of Bath, Bath BA2 7AY, UK

A study has been made of the effect of prior damage on the tensile strength and toughness of a number of carbon and glass fibre reinforced plastics materials. The methods of introducing this prior damage were by tension fatigue cycling, by transverse compression, by repeated impact, and by stress corrosion. The effects of the damage were assessed by measuring the un-notched and notched tensile strengths and, in some instances, the work of fracture of notched samples. Acoustic emission monitoring and microstructural studies were carried out in support of the mechanical tests. It appears that under various circumstances, the effects of microstructural damage may result in independent changes in the notched and un-notched strengths of a composite, although the pattern of changes is not simple. The toughness to strength ratio, K_Q/σ_f, may rise or fall, depending on the material and the damaging conditions. However, the results for all of the tests presented here still fall within the 90% confidence limits for the K_Q/σ_f relationship previously identified.

1. Introduction

There are several approaches to the problem of calculating the strength of notched (i.e. "defective") composites. These include methods which rely on the determination of the state of stress, either at a specific point or over a given volume, ahead of a stress concentrator [1–3], and the application of linear elastic fracture mechanics methods for the determination of critical stress intensity factors [4–6]. Both methods appear to have been successful in various ways for the prediction of notched strength of various composite materials, provided certain specific factors relating to the microstructural peculiarities of fibre composites are taken into account. In a recent paper [7], Wetherold and Mahmoud explored the applicability of both approaches to a set of experimental results obtained from eight varieties of fibre composites, including both thermoset and thermoplastic matrices, different volume fractions of glass, carbon, and mixed fibre reinforcements, continuous and short fibres, and different processing methods. They concluded that the basic single-parameter point stress model [1, 2] and the more complex two-parameter model [3] gave good agreement with their experimental results provided the parameters were regarded as material-specific constants rather than universal constants. Similarly, fracture mechanics methods only gave satisfactory agreement if some small-scale yielding or damage parameter, again material-specific, was used, thus confirming an earlier proposal by Dorey [5, 6]. Wetherold and Mahmoud also showed that there was good correlation (with correlation coefficient, $r = 0.992$ for eight data pairs) between the un-notched tensile strength, σ_f, and the candidate fracture toughness, K_Q, of the form

$$K_Q = 0.66\sigma_f - 3.36 \quad (1)$$

where the units of stress are 10^3 lbf in^{-2} and those of K_Q are 10^3 lbf in$^{-3/2}$. In fact there seems to be no logical reason for not forcing the relationship through the origin, and the result, reverting now to SI units (MPa and MPa m$^{1/2}$) is equivalent to

$$K_Q/\sigma_f \approx 80\,(\mu m)^{1/2}$$

Shortly after the appearance of this paper, Harris *et al.* [8] reported on a survey of results published over a twenty year period for an even wider range of composites (67 data pairs). From this survey, which was restricted to values of strength and K_Q determined in tension, it was shown that there was apparently a linear relationship, in SI units as defined earlier, of the form

$$K_Q \approx 64\sigma_f \quad (2)$$

Although the slope of this relationship is lower than that of Wetherold and Mahmoud, their experimental results actually fall within the scatterband of all data pairs included in the survey of Harris *et al.* (90% of all data within $\pm$ 14 MPa m$^{1/2}$ on the K_Q axis) and it should be borne in mind that few of those results had been corrected for "process zone size" in the manner of Dorey and of Wetherold and Mahmoud. More recently, an independent study by Belzunce *et al.* [9] on chopped strand mat and woven cloth reinforced GRP produced further results that closely fitted Equation 2.

This is of course the inverse of what is commonly found for metallic materials, and it runs contrary to the commonly held belief that the strength of com-

0022–2461/91 $03.00 + .12

TABLE I Tensile properties of GRP and CFRP laminates

Composite	Type	Modulus (GPa)	Strength (GPa)	Failure strain (%)	Toughness[a]
XAS carbon–epoxy	prepreg[b]	76	1.17	1.47	67 MPa $m^{1/2}$
XAS carbon–epoxy	prepreg[c]	70	1.01	1.47	52 MPa $m^{1/2}$
T300 carbon–epoxy	prepreg[d]	53	0.76	1.50	50 MPa $m^{1/2}$
E-glass–epoxy	prepreg	24	0.53	2.11	36 MPa $m^{1/2}$
WR E-glass–epoxy	prepreg	29	0.28	2.50	18.6 kJ m^{-2}
CSM–polyester	RTM	20	0.26	2.50	16.6 kJ m^{-2}

[a] First four values are K_Q values, and the last two are fracture energies.
[b] batch 1 used for transverse compression studies.
[c] batch 2 used for fatigue damage studies.
[d] batch 3 used for repeated impact experiments.

posites is independent of fracture toughness [10–12]. The implication of this result is that all composites reinforced with conventional fibres (i.e. those with diameters of about 10 μm) appear to behave as though they contained defects about 1 mm in size [4] (which is of the order of dimension of a chain of fractures of 100 to 150 fibres, or the cross-section of a 10 000 fibre tow) no matter what their structure or composition. This seems unlikely, and it was, therefore, concluded that the use of the critical stress intensity concept has no meaning for such materials on account of their complex structure and cracking patterns. It, nevertheless, raises interesting questions about the degree of interdependence of the notched and un-notched strengths of fibre composites and the extent to which there is any scope for modifying the toughness of a composite independently of its tensile strength, a concept that has commonly been accepted not only as feasible, but as a vital part of the design of a component to meet specific requirements.

Since our earlier work [8] indicated that familiar materials variables such as matrix resin, fibre type, volume fraction and distribution, and manufacturing method do not bring about independent changes of the two properties, we have attempted to make a study of the effects of prior structural damage. It is frequently stated [5, 6, 13] that different composite lay-ups exhibit different levels of toughness on account of the way in which microstructural damage is affected by composite structure and the manner in which it interacts with growing cracks. We have, therefore, carried out a series of experiments deliberately to introduce damage of various kinds into both glass and carbon fibre reinforced plastics composites (GRP and CFRP) in order to assess its effect on strength and "toughness".

2. Experimental details

2.1. Materials

Various kinds of composite have been used in this work, including autoclaved GRP and CFRP laminates manufactured from prepreg materials, woven-roving GRP laminates, and resin transfer moulded chopped strand mat–polyester material. The prepreg materials were carbon and glass fibre reinforced epoxy laminates containing a combination of 0° and ±45° plies. Two batches of CFRP samples were of $[(\pm 45, 0_2)_2]_s$ construction and consisted of Courtauld's XAS fibres in Ciba-Geigy BSL913 and 914 epoxide matrices, while the third was a quasi-isotropic $(+45, 0, -45, 90)_{2s}$ material consisting of Toray T300 fibres in a 914 resin. The GRP group included a number of samples of $(0, -45, +45, 0_2, +45, -45, 0)_s$ and $(+45, 0_2, -45, +45, 0_2, -45)_s$ construction in addition to $[(\pm 45, 0_2)_2]_s$, but all were of E-glass in Ciba-Geigy BSL913 resin. These three lay-ups showed no differences in mechanical behaviour, and all GRP results have, therefore, been pooled. The materials were autoclaved, following the manufacturer's instructions, from zero-bleed prepregs to produce laminates approximately 2 mm thick with a nominal fibre volume fraction of 0.60. Test strips 200 mm long by 20 mm wide were cut from the pressed plates and soft aluminium end tabs were glued on prior to mechanical testing.

The woven-roving GRP laminate was a 6.2 mm thick, press-laminated Permali Permaglass 22FE/25 plate containing 35 layers of mixed coarse- and fine-weave cloth in a conventional bisphenol-A/DDS/DDM resin system ($V_f \approx 0.47$). The CSM plates were resin transfer moulded from E-glass mat and Scott Bader Crystic C199 polyester resin: they were approximately 4.2 mm thick and of 0.29 fibre volume fraction. The basic mechanical properties of undamaged samples of these various materials are given in Table I.

2.2. Methods of introducing damage

2.2.1. Fatigue damage

Samples of CFRP were subjected to repeated tension fatigue cycling in Instron 1300 series servo-hydraulic machines under load control at a frequency of 5 Hz (10 Hz for the longest tests) and an R ratio of +0.1. These fatigue tests were carried out on straight-sided (unwaisted) test coupons, with their edges polished to permit edge replication studies of damage by means of optical microscopy, and with soft aluminium end-tabs bonded on to prevent grip damage. The characteristic stress–log life ($S/\log N$) curve for the CFRP laminate is given in Fig. 1. The development of early fatigue damage in one sample was monitored by acoustic emission (AE) analysis with equipment and methods described in earlier papers [14, 15]. For this purpose it was necessary to carry out the cyclic loading in a

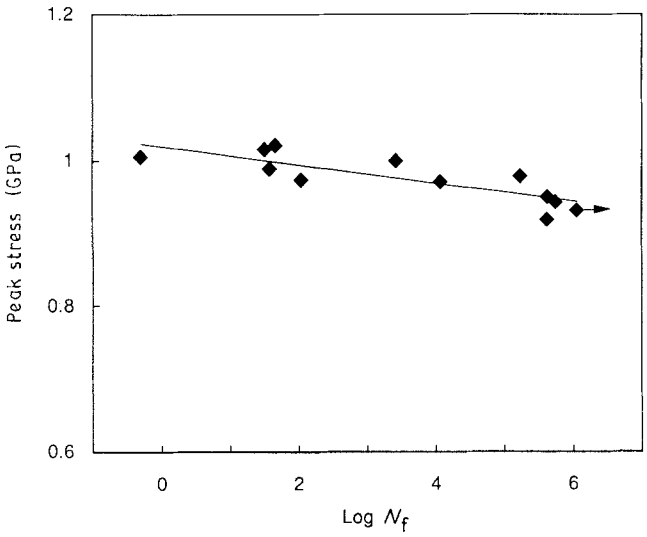

Figure 1 Stress–log life data for $[(\pm 45, 0_2)_2]_s$ XAS–914 CFRP composites fatigue tested in repeated tension at an R ratio of $+0.1$.

screw-driven Instron machine running at approximately 1 Hz.

The damage induced by fatigue loading of a $[(\pm 45, 0_2)_2]_s$ laminate is inevitably complex and includes fibre breakage, resin and interface cracking in the $\pm 45°$ plies and, in the later stages of cycling, delaminations developing from edges and from points of crossover of cracks in differently oriented plies. A detailed study of the individual damage mechanisms contributing to the deterioration of the $[(\pm 45, 0_2)_2]_s$ CFRP laminate under fatigue conditions is to be published separately.

The fatigue damaged samples were then tested in tension to establish their un-notched and notched tensile strengths, the latter from test pieces with a notch-to-depth ratio, $2a/W$, of 1/3. The edge notches were cut with a jeweller's saw and sharpened with a scalpel. Some of these mechanical tests were also accompanied by acoustic emission monitoring.

2.2.2. Transverse compression

The autoclaved CFRP and GRP composites were subjected to damage by transverse loading in compression to various fractions of the fracture load for this mode of deformation. The transverse loads were applied in a plane strain compression jig of conventional design, the press tools, of various widths, being sufficiently long to extend well beyond the sample width (Fig. 2). The damage zones which were thus created in the centre of the specimen test lengths were expected to contain a complex mixture of damage, including resin deformation and cracking, interfacial shearing, and fibre fracture. Notched and un-notched strengths of the damaged samples were again measured, as described above, the edge notches, in this case, being cut along the centre lines of the damaged zones.

2.2.3. Repeated impact damage

These experiments were carried out on the thicker GRP laminates and the quasi-isotropic CFRP. Prepared samples were held in close contact with a rigid steel anvil bolted into an Avery–Denison pendulum impact machine and were damaged by repeated impacts from the tup which had a 20 mm diameter striker of semicylindrical shape in place of the usual sharp-fronted impacter. The maximum height from which the tup was released was 500 mm, which produced an incident impact energy of 10 J, the energy level that might be associated with the dropping of a 1 kg spanner from waist height. The tup rebounded from the composite after impact, with the result that some 15 to 20% of the incident energy was unabsorbed at each impact.

The line of contact of blows delivered by the striker was, therefore, again perpendicular to the sample long axis. This method is different from the conventional method of carrying out repeated impact studies where the sample is not fully supported. Levels of damage experienced in such tests are usually much greater because of the high flexural and shear stresses imposed, in addition to the in-plane tensile stresses that occur if positive end-clamping is used. The total absorbed energy comprises several separate components, the relative magnitudes of which depend on both composite and test parameters, as discussed, for example, by Morton and Goodwin [16]. In our fully supported test geometry, the damage is largely due to local ("Hertzian") contact forces, and will include matrix plastic deformation and cracking and fibre

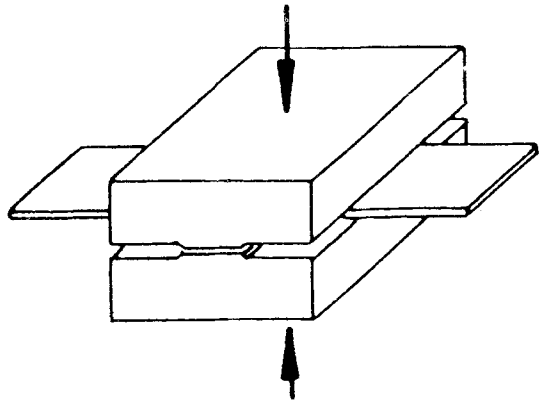

Figure 2 Method of inducing transverse compression damage with a plane-strain compression jig.

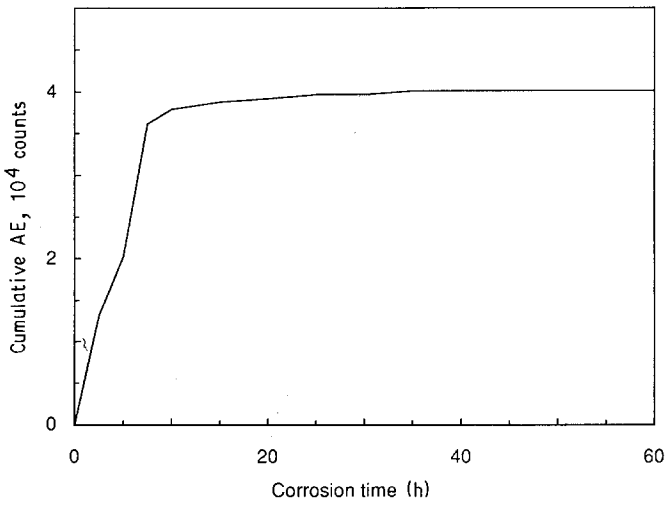

Figure 3 Acoustic emission ringdown counts plotted against time for a $[(\pm 45, 0_2)_2]_s$ GRP sample bent so as to induce a tensile strain of 0.2% while exposed to 5N HCl solution.

fracture, but little or no delamination. The GRP in the contact zone showed clear evidence of stress whitening: in samples subjected to extensive double-sided impact this whitening occupied the whole sample cross-section. Typically, the threshold for barely visible impact damage (BVID) was 25 J.

Samples were damaged to various cumulative levels of absorbed energy, and the effect of this on the notched strength (CFRP) or the work of fracture (the total energy absorbed during the failure of a notched sample in a Charpy test – for the thicker GRP) was assessed for both single-sided and double-sided impact. The usual method of assessing the effects of the substantial levels of delamination that occur in repeated impact tests on unsupported samples is the measurement of longitudinal compression strength. Delamination was not, however, a major damage mode in our fully supported impact tests.

To afford a comparison with the transverse compression experiments on the thinner laminates, a number of the woven-roving GRP samples were also damaged by transverse compression to increasing proportions of the transverse compression failure load using, in this case, a 20 mm diameter bar to load the sample against a flat anvil, rather than the plane strain compression geometry of Fig. 2. Tan and Sun [17] have shown that for CFRP materials containing 0° and 45° plies the low velocity impact indentation behaviour may be adequately described by statical contact laws obtained by adapting Hertzian models (see Willis [18], for example) for thin plates of anisotropic materials. Consequently, any differences in behaviour between statical transverse compression and impact, for similar indenter geometries, must presumably stem from strain-rate dependent behaviour of the matrix resin.

2.2.4. Stress corrosion

Some GRP samples were damaged by stress corrosion cracking. Strips of the laminate were bent elastically in simple jigs to a radius corresponding to a maximum tensile strain of 0.2%, approximately a tenth of the flexural failure strain. They were then immersed in 5N HCl solution for various times during which acoustic emission monitoring indicated the occurrence of substantial amounts of fibre damage, possibly with some resin cracking, as illustrated for pultruded glass–epoxy rods under similar conditions [17]. Stress corrosion damage was accompanied by a rapid evolution of acoustic emission over an initial period of about 10 h, indicating substantial damage to the fibres in the outer $\pm 45°$ plies, followed by an approach to saturation damage reached after about 50 h (Fig. 3). The cumulative ring-down count level associated with this damaged state was about 4×10^4. Other damage mechanisms would have been unlikely to occur under these conditions. Following corrosion, the notched and un-notched strengths of the damaged samples were measured.

2.3. Acoustic emission monitoring

The monitoring of acoustic emission in the various experiments described above was carried out with an AETC Corporation Amplitude Analysis System and data acquisition equipment which has been fully described elsewhere [11, 12]. This is a 50 channel system, each channel being of 1.2 dB band width, and for the purposes of easy evaluation of the shapes of the amplitude histograms provided by the equipment the channels are lumped so as to give bands of low (channels 1 to 10), intermediate (channels 11 to 20), and high (channels 21 and above) amplitudes. Graphs are then plotted of the percentage share of the total number of events at any given point appearing in these three channels. This very crude level of resolution is usually sufficient to indicate significant changes in the shape of the amplitude distribution, and the normalization process eliminates difficulties of interpretation resulting from major variations in the overall total numbers of counts.

3. Experimental results

3.1. Fatigue damage

Changes in stiffness, tensile strength, and notched strength resulting from repeated tension cycling are shown in Fig. 4a, b and c. It can be seen that for cyclic (peak) stress levels between about 65 and 95% of the mean monotonic tensile strength, reductions in Young's modulus and strength, following initial small

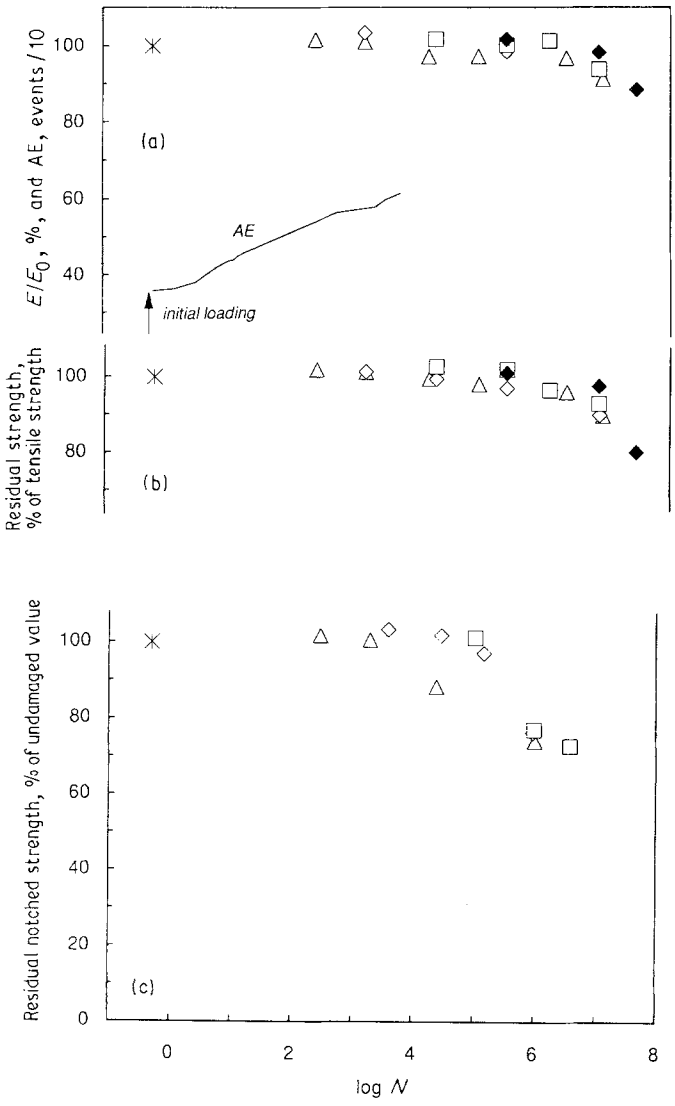

Figure 4 Residual mechanical properties of $[(\pm 45, 0_2)_2]_s$ CFRP laminate as a function of number of fatigue cycles following cycling at 5 Hz and $R = +0.1$. (cyclic stress level, % of failure stress: △93, ◇86, □76, ◆68) (a) Young's modulus, (b) residual tensile strength, (c) residual notched tensile strength. (cyclic stress level, % of failure stress: △90, ◇78, □66). All data are normalized with respect to the initial (undamaged) values. The superposed acoustic emission results in (a) were obtained by incremental cycling of a single test sample at 1 Hz.

increases of 1% or 2% are of the order of only 20% even after 10^6 cycles. No significant reductions occur until well beyond 10^4 cycles, even though in the early stages of life cycling is accompanied by a continuing increase in the cumulative number of acoustic emissions, as shown in Fig. 4a, from which it can be seen that over the first 1600 cycles of a fatigue test at 76% of the failure stress the cumulative number of AE events continued to increase during the early stages of life when no deterioration of mechanical properties could be detected. Acoustic emission amplitude histograms for the first loading cycle and subsequent cumulative histograms for cycles 2 to 10, 12 to 200, 200 to 700, 700 to 1000, and 1300 to 1600 were analysed in the way described earlier, and the results are shown in Fig. 5. No significant changes occur in the high energy band, the proportion of counts above channel 20 (24 dB above threshold) being very small, but there are relative shifts of activity between the low and intermediate amplitude bands. The predominant band is

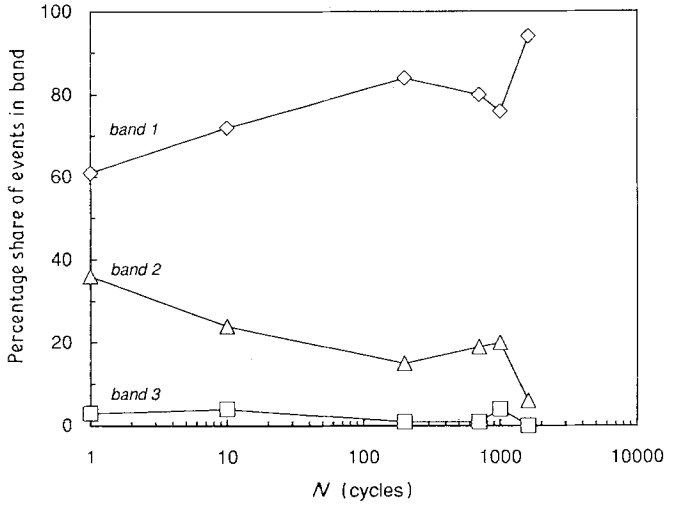

Figure 5 Changes in the acoustic emission amplitude distribution during cycling of $[(\pm 45, 0_2)_2]_s$ CFRP laminate. The curves indicate the percentage share of emissions falling in three broad amplitude bands: band 1 = amplitudes 0 to 12 dB (above threshold); band 2 = 13 to 24 dB; band 3 = all events above 25 dB.

always the lowest amplitude group (0 to 12 dB), but the fact that there are changes in the distribution suggests variations in the rate of occurrence of at least two localized damage mechanisms even though these are not associated with macroscopic property changes. Over the first hundred or so cycles, the proportion of events in band 1 rises from some 60% after one cycle to a level of 80% which is characteristic of the response of a sample loaded in monotonic tension to failure (see Fig. 9, later). There is a corresponding change in band 2, but very little change in the numbers of events in band 3 in which there is, in any case, relatively little activity. The significant changes in the amplitude distribution come in the vicinity of 1000 cycles when, after a slight fall in the proportion of band 1 activity, there is a marked rise in the fraction of low amplitude events, up to more than 90% when monitoring was discontinued, with very little residual activity in both of the other bands. This marked change in behaviour is matched by observations from edge replication tests which show that beyond 1000 cycles there is the first visible evidence of fibre fractures in the 0° plies and resin cracks in the $\pm 45°$ plies. Despite common prejudices [18, 19] that commonly relate only high-amplitude AE events with fibre failure, the rise in the incidence of activity in the low amplitude band towards 10^4 cycles when all observed mechanical properties begin to be adversely affected, suggests that these low amplitude events are associated with random failure of fibres in the 0° plies. The reason for the initial rise and fall of activity in the low amplitude band, and the associated changes in band 2, is less clear since no visible signs of damage were revealed by edge replication in this region of cycling.

Residual stiffness and strength vary together in such a way that the tensile failure strain of the material remains unchanged by the fatigue damage, as confirmed by failure strain measurements and as expected for a fatigue process where composite failure strain determines the overall fatigue failure process. Although there is some indication, when the data of Fig. 4a and b are plotted on a larger scale, that the degrees of reduction in strength and stiffness are greater the higher the cyclic stress level, these differences are small and within the normal level of variability of mechanical properties. It can be seen from Fig. 4c, however, that the reduction in notched strength is somewhat greater and more sensitive to cyclic stress level. Since the geometry of the notched tensile test samples was invariable, the fractional change in the notched strength is identical with the change in fracture mechanics parameters such as K_Q and K_{Ic} that would normally be calculated from the notched strength data. Discussion of the results in terms of notched strength, therefore, avoids philosophical difficulties relating to the application of fracture mechanics to composites.

3.2. Transverse compression damage

The damage induced by transverse compression resulted in some minor permanent changes in shape of the sample cross-section in the damage zone. In the CFRP, microstructural examination revealed matrix plastic deformation, with local bending of fibres, matrix cracking and substantial fibre breakage in both 0° and 45° plies, some of the former being directly attributable to the effects of matrix cracks in neighbouring plies. A collage of typical damage mechanisms observed in these transversely loaded CFRP samples is presented in Fig. 6.

By contrast with the CFRP, and despite the high levels of deformation, the GRP laminates showed no visible signs of either fibre breakage or matrix cracking, presumably because of the higher failure strain and lower stiffness of the glass fibres by comparison with those of the carbon. The AE patterns obtained from un-notched tensile tests on the GRP showed no dramatic changes as a result of the transverse damage, although there was some indication that the AE activity in the early stages of the tests was slightly higher in damaged samples than in undamaged ones (Fig. 7). For the CFRP, however, there was a much clearer indication of the effects of damage, Fig. 8 showing both an increase in the overall AE levels at failure with increase in transverse compression load level and, for a given transverse load, with the area of the damaged region. The wider the damaged zone, however, the more variable were the AE results. The changes in the AE amplitude distribution during the tensile testing of undamaged and damaged samples are shown in Fig. 9. The results from the three samples represented, which are plotted in terms of the duration of the test, show similar changes in the relative distribution of low and intermediate amplitudes with increasing load, and no progressive trend with increase in the level of prior damage sustained by the samples. By and large, the stable form of these distributions, following the initial settling in period, is about 80% of events in band 1 and 20% in band 2, with very few events in the range of amplitudes above 25 dB (above threshold). This distribution is similar to those observed elsewhere for a range of composite types loaded to failure in tension [15]. The prior level of damage does not appear to change the nature of the damage mechanisms during subsequent tensile loading.

Fig. 10 shows the effect of transverse compression on the un-notched and notched strengths of the GRP laminates. The mean undamaged strength and K_Q values for the GRP were 529 MPa and 36 MPa $m^{1/2}$, respectively, with coefficients of variation of 7 and 4%. For transverse compression loads close to failure (90% of maximum) the strength is only marginally reduced, while beyond a damage level of about 50%, the notched strength appears to rise by some 30%. Thus although the initial value of 67 (units of $\mu m^{1/2}$) for the ratio K_Q/σ_f is close to the value of 64 given by Equation 2, it is about 50% greater than this ($K_Q/\sigma_f \approx 100$) after the most severe compression damage. In this case, therefore, the strength and fracture toughness appear to change relative to each other, in the opposite manner to that implied by Equation 2. Conceptually, in conventional fracture mechanics terms this change implies an increase in the critical defect size, although by a factor of less than 2.

By contrast, the CFRP laminate was much less

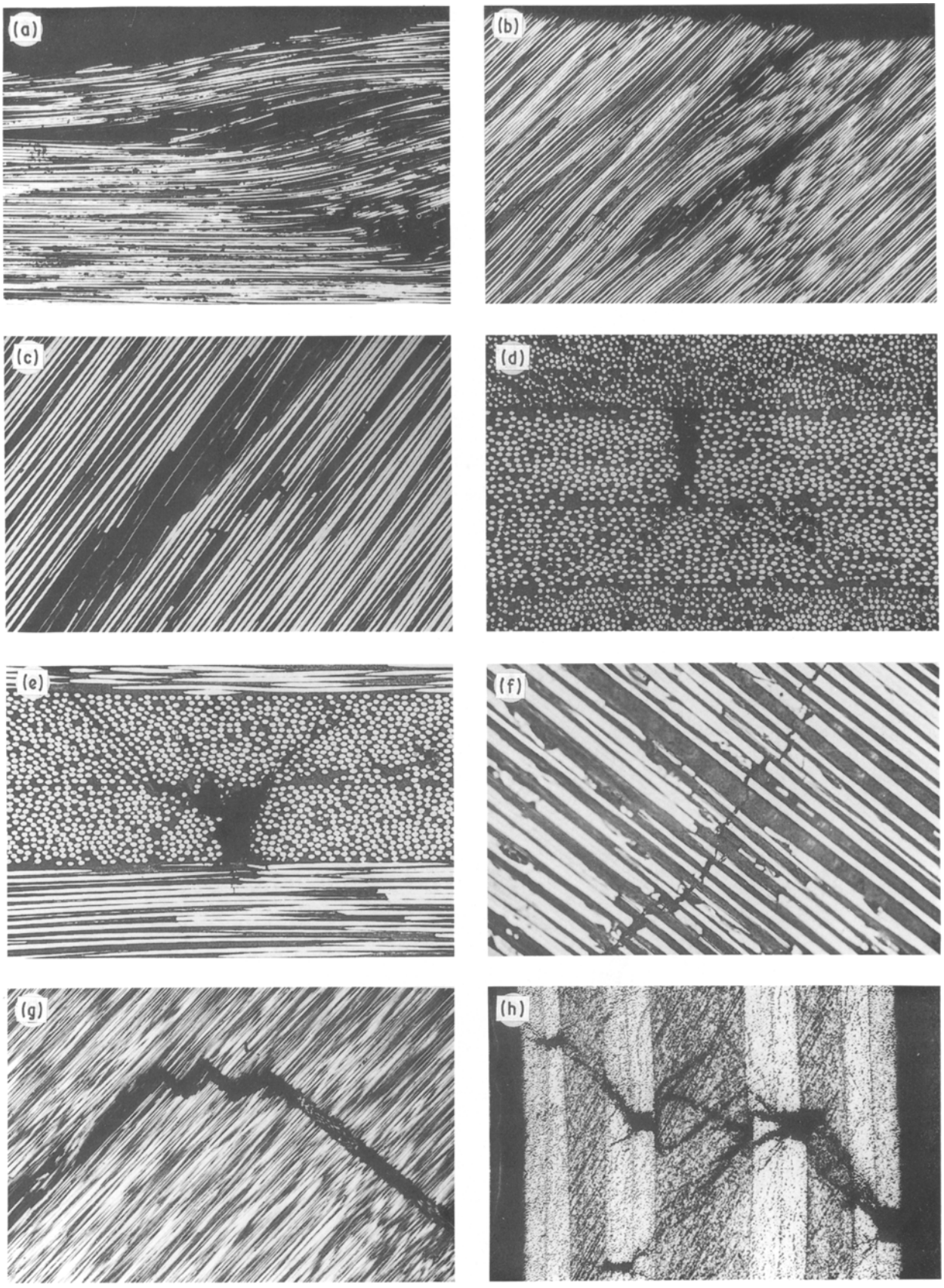

Figure 6 Modes of damage observed in $[(\pm 45, 0_2)_2]_s$ CFRP laminate following transverse compression between plane strain compression platens. (a) plastic squeezing and deformation of resin and some fibre breaks in an internal 0° ply (b) similar to (a) but in a 45° ply (c) matrix crack and neighbouring fibre breaks in a 45° ply (d) longitudinal matrix crack in an internal 45° ply (e) a 45° ply crack, tensile + shear, with associated fibre breaks in an adjacent 0° ply (f) fibre breaks in a +45° ply adjacent to a longitudinal crack in the underlying −45° ply. (g) linking between a longitudinal matrix crack and a crack normal to the fibres (h) through-thickness shear damage patterns linking the various features illustrated in earlier pictures.

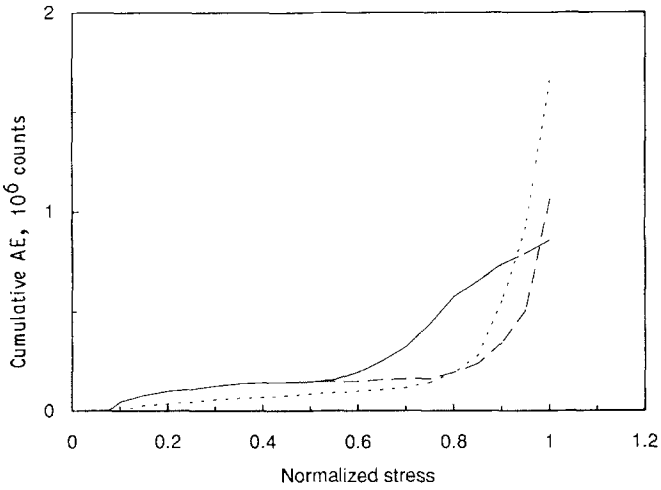

Figure 7 Cumulative AE ringdown counts vs stress during tensile tests on undamaged (----) and damaged GRP laminates (transverse compression damage) (—— 85% damage, – – – 80% damage). The stress is normalized with respect to the failure stress.

strongly affected by the transverse compression. Fig. 11 compares the fractional changes in notched strength for both GRP and CFRP, and it can be seen that the apparent toughness of the CFRP remains unaffected until transverse damage levels as high as 95% of the failure level. For the CFRP, the transverse stress at which catastrophic crushing occurred was about 1 GPa for 10 mm wide platens and 10% lower for 20 mm wide platens (the difference presumably being due to the familiar "friction hill" pressure concentration under plane platens which could not be

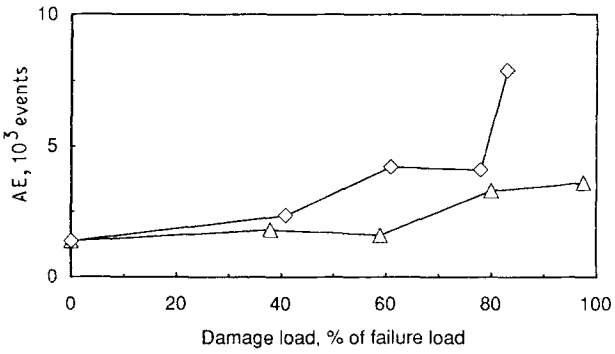

Figure 8 Total AE events at failure as a function of transverse compressive damage load (normalized with respect to transverse compression failure load) for the CFRP laminate. (◇ 20 mm wide platens, △ 10 mm wide platens).

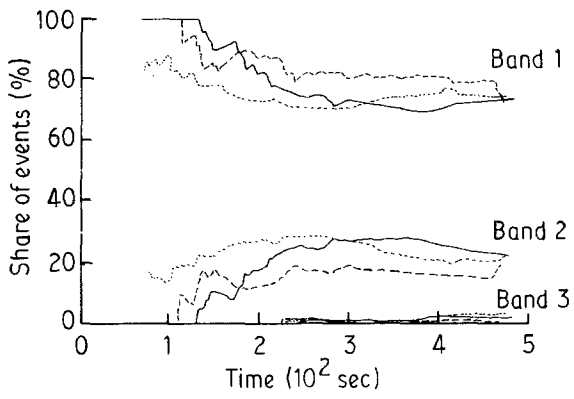

Figure 9 Changes in the acoustic emission amplitude distribution (percentage share graphs) for $[(\pm 45, 0_2)_2]_s$ CFRP samples following transverse loading to various compression stress levels (—— no damage, ----- 80% compression, – – – 90% compression).

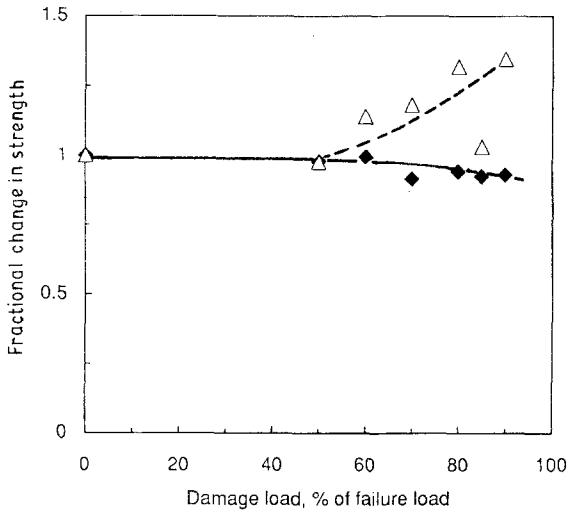

Figure 10 Variation of the notched (△) and un-notched (◆) tensile strengths of $[(\pm 45, 0_2)_2]_s$ GRP laminate as a function of transverse damage load. The strengths are normalized with respect to undamaged values and the transverse damage loads with respect to the transverse failure load.

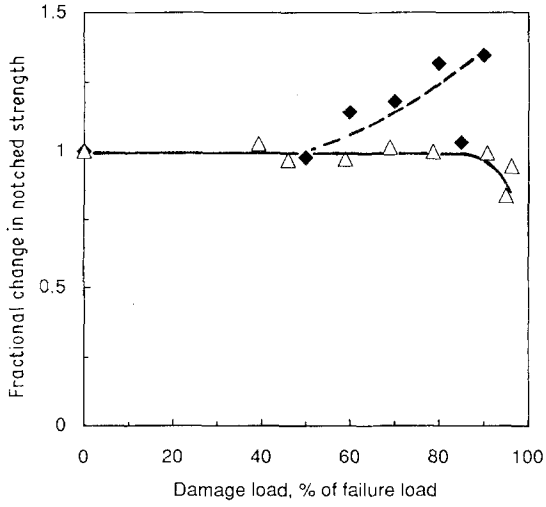

Figure 11 Comparison of the effects of transverse damage on the notched strengths of $[(\pm 45, 0_2)_2]_s$ GRP (◆) and CFRP (△) laminates.

eliminated in these experiments). The value of K_Q for the undamaged CFRP was 67 MPa $m^{1/2}$ (cv $\approx$ 5%), and the small variations of K_Q with damage below 90% all fall within the undamaged scatterband. The CFRP datum points in Fig. 11 include tests with both 20 and 10 mm wide platens, but there is no clear distinction between them. At the 95% damage level, the 20 mm wide tools gave a reduction in toughness of 16% to 56 MPa $m^{1/2}$, by comparison with a reduction of only 6% for 96% damage with the 10 mm wide tools. This slight drop in apparent toughness was accompanied by a somewhat greater reduction in tensile strength, but again only for damage levels in excess of 90%. The measured tensile strength for 91% damage was 0.72 GPa and the ratio K_Q/σ_f was therefore increased, by the highest levels of compression damage, to 92 from a starting point of 62 for undamaged material.

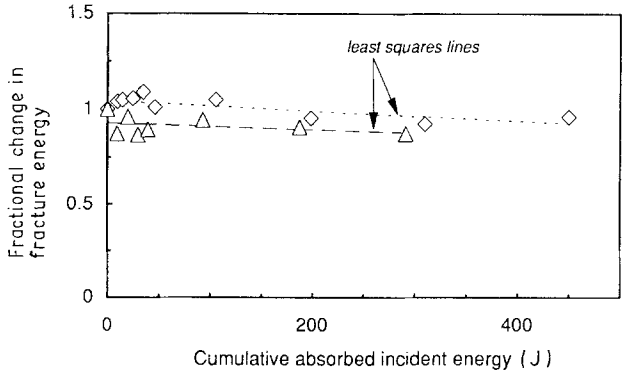

Figure 12 Effect of repeated impact on the work of fracture of woven-roving glass/epoxy composite. Results for both single (◇) and double-sided (△) impact.

3.3. Repeated impact damage

For this part of the work we have tried to assess the effect of localized impact damage on the fracture energy in order to afford a comparison with the notched strength behaviour described in previous sections. The damage experiments can be carried out in two ways, either by impacting one side of the sample only, or by reversing the sample after each impact in order to cause a more symmetric distribution of damage. Apart from the relatively small dent caused by the cylindrical impacter at the point of contact, polished cross-sections of the damaged zones revealed relatively little direct evidence of the expected effects of repeated impact in the stress-whitened zone. The only indications of damage were some fibre breaks occurring in the 0° warp fibres close to the adjacent weft fibres at points of cross-over in the weave, and very localized delaminations between perpendicularly oriented fibre tows, again at weave-crossover points. Since the matrix was not found to be cracked, contrary to expectation, the stress whitening must presumably have resulted either from fibre–matrix interfacial shearing movements or from resin plastic deformation. The signs of damage in cross-sections of WR glass–epoxy samples loaded in compression with the cylindrical indenter were similar to those in the impacted sample.

As Fig. 12 shows, for a given total absorbed energy, double-sided impact results in a somewhat greater initial reduction in toughness than single-sided impact. The subsequent rates of fall of fracture energy, however, indicated by the least squares lines in the figure, are little different, indicative of the high damage tolerance of this woven-roving GRP composite. Despite the damage to the 0° fibres shown in Fig. 12, the strength is also largely unaffected by the impact damage. Fig. 13 shows that the fractional changes in both fracture energy and un-notched strength of this material are little affected by sustained repeated impacts, despite the marked stress whitening and loss of translucency in the damage zone. The lower volume fraction CSM composite also appeared relatively resistant to repeated impact although, as Fig. 14 shows, the least squares line has a slightly steeper slope than that for the WR composite. This small difference presumably reflects the slightly higher resin content of the CSM material.

In view of the uncertainty about the difference between the damage caused by impact and by sustained loads, we carried out one set of experiments on the woven-roving GRP laminate in which transverse damage was induced by slow compression loading using the same loading geometry (semicylindrical indenter; solid back support) as that used for the repeated impact. A direct comparison in terms of absorbed energy is not possible, but the results are presented in Fig. 15 in terms of the load level applied by the cylindrical indenter as a percentage of the load required to cause catastrophic, crushing–penetrative failure (c.f. Fig. 10). It can be seen that the reduction in fracture energy caused by loading to nearly 90% of the crushing load is slight and of the same order as that produced by single-sided impact to nearly 500 J of absorbed energy, by contrast with the plane strain compression of the $[(\pm 45, 0_2)_2]_s$ GRP laminate where there was a slight increase in the notched tensile strength.

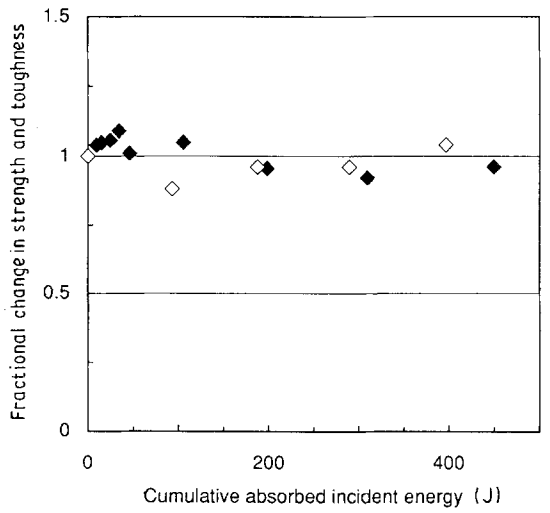

Figure 13 Effect of repeated impact (single-sided) on the work of fracture and un-notched tensile strength of WR glass–epoxy laminate (◆ toughness, ◇ strength).

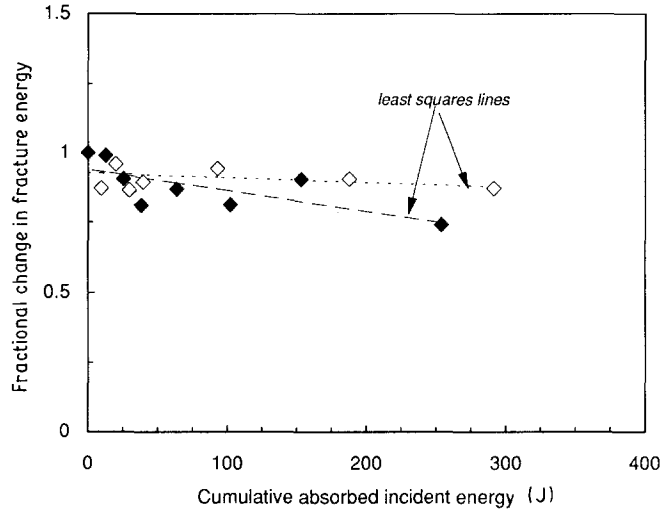

Figure 14 Effect of repeated impact (double-sided) on the work of fracture of WR glass–epoxy and CSM glass–polyester composites (◇ WR, ◆ CSM).

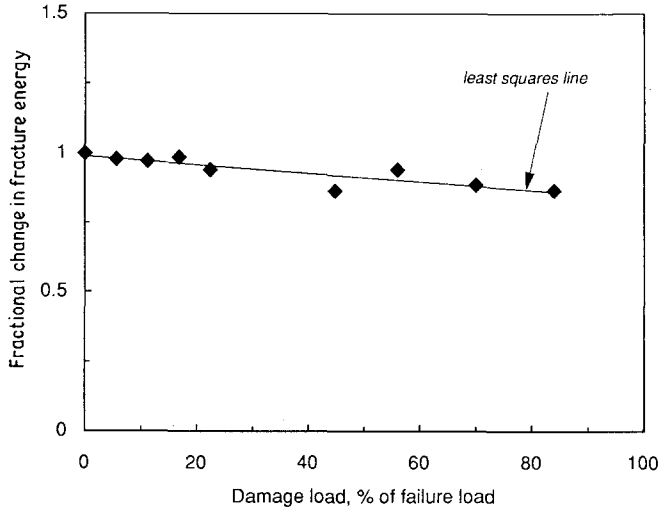

Figure 15 Effect of transverse compression by cylindrical indenter on the work of fracture of WR glass–epoxy composites.

By contrast with the GRP materials, the CFRP laminate was far less resistant to repeated impact, apparently losing up to 50% of its notched strength by energy levels of only 250 J (Fig. 16), compared with almost no loss in fracture energy of the WR GRP laminate damaged to twice this level. Dorey *et al.* [22] report similar levels of loss of un-notched tensile strength for a similar CFRP composite of identical layup and thickness in unsupported repeated impact tests after only 8 J of incident energy. Unfortunately, insufficient material was available for determinations of the tensile strength of the CFRP damaged by repeated impact although, as in the case of the plane strain compression, no loss in strength occurred after slow loading with the same indenter to about 50% of the transverse failure load.

3.4. Stress corrosion effects

AE monitoring of un-notched tensile tests on GRP samples damaged by stress corrosion revealed far

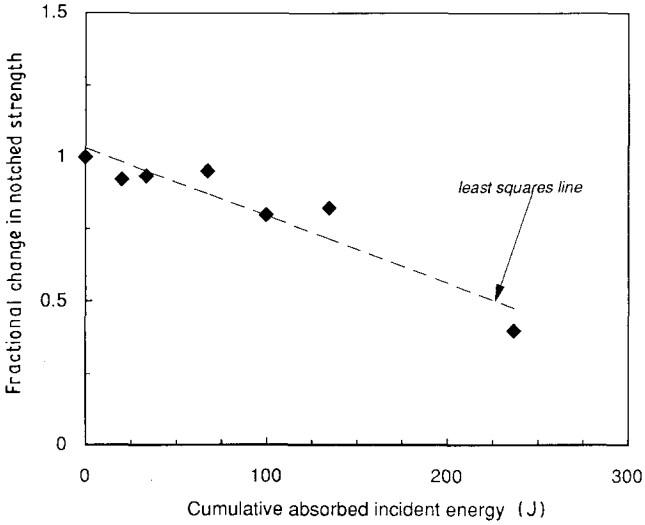

Figure 16 Effect of repeated impact (double-sided) on the notched strength of CFRP laminate.

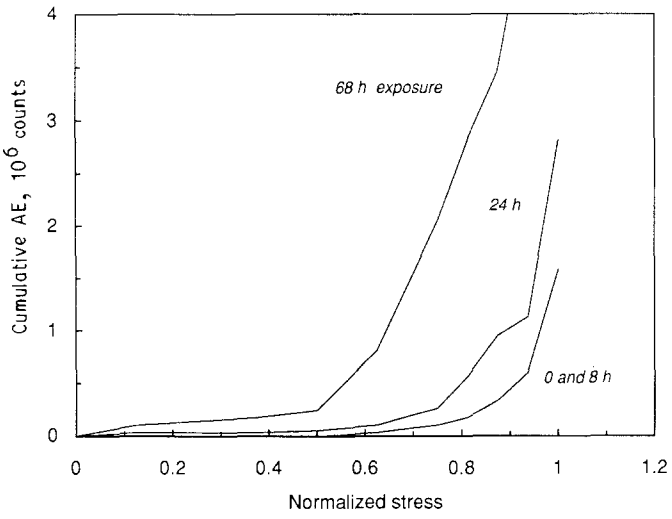

Figure 17 Cumulative AE ringdown counts plotted against normalized stress during tensile testing of stress-corroded GRP samples.

more marked effects than had been found following transverse compression.

Fig. 17 shows that an exposure of 8 h does not alter the variation of AE activity with loading during tensile loading to failure, whereas further increases in exposure time result in increasingly high overall levels of AE output and at increasingly lower strain levels. These effects give more definite indication of the increasing damage levels in the corroded samples than in the case of transverse compression damage. The corrosion damage has also resulted in almost complete elimination of the AE threshold characteristic of undamaged material. However, the changes in strength and apparent toughness brought about by this obvious corrosion damage were even less marked than those for transverse compression, as Fig. 18 shows. The changes in strength, again only marginally outside the undamaged scatter band, indicate a small overall decrease, while the corresponding notched strength values show no significant net change. The K_Q/σ_f ratio, therefore, shows only a slightly rising trend with increasing damage level, as indicated by the least squares line in Fig. 18.

4. Discussion

Taking the notched and un-notched strengths of the CFRP laminate as an example, we note that the ratio of these two properties, σ_N/σ_f, for the undamaged material was 0.66. Applying the familiar sample width correction factor [21], $[(W/\pi a)\tan(\pi a/W)]^{1/2}$ which amounts to 5% for our sample geometry, the corrected value of this ratio, σ_N^∞/σ_f, is then 0.693. The exact anisotropic elasticity solution [1] for the normal stress distribution ahead of a crack in a plate under uniform tensile stress, σ, leads to the point stress failure criterion for a notched sample of finite width:

$$\sigma_N^\infty/\sigma_f = (1 - f^2)^{1/2} \quad (3)$$

where $f = a/(a + d_0)$, a being the notch length and d_0 the characteristic fixed distance ahead of the notch at which the local stress reaches the un-notched composite strength. The equality in Equation 3 is satisfied if d_0 is equal to 1.29 mm, as discussed in the Introduction and in references [3, 5, 6].

The data of Fig. 4a, b and c are combined in Fig. 19 to show the effect of cycling at different peak tensile stress levels on the ratio σ_N/σ_f. It can be seen that there is no change in the value of this ratio over the first 10^4 cycles, whatever the cyclic tensile stress. Beyond this, however, the more rapid deterioration in the residual notched strength results in a downward shift of the σ_N/σ_f ratio (or the K_Q/σ_f ratio), this reduction occurring at about the same number of reversals for cyclic stresses of 67% and 77% of the failure stress, but significantly earlier for 93%. The simplest explanation

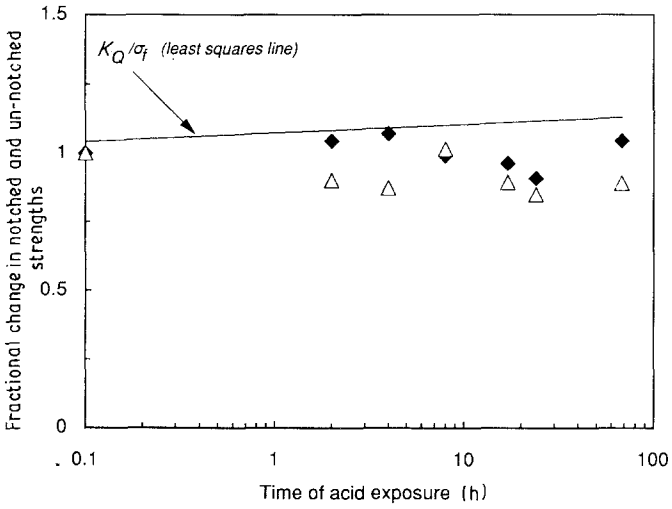

Figure 18 Effect of stress corrosion on the notched (◆) and un-notched (△) strengths of GRP laminate (normalized strength data).

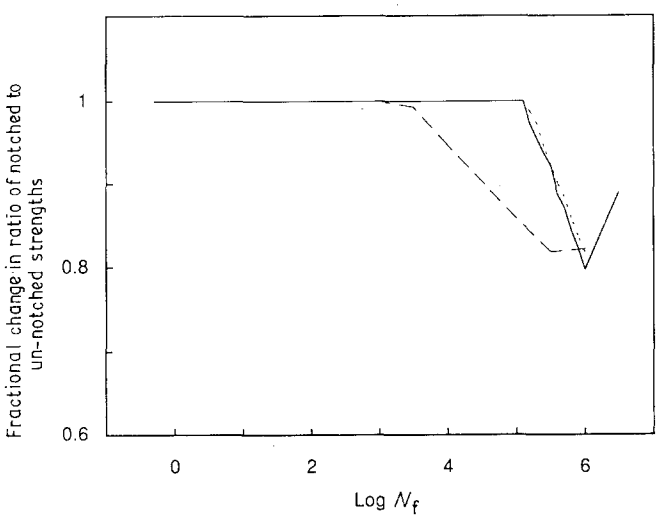

Figure 19 Ratio of normalized notched and un-notched strengths following repeated tension cycling of $[(\pm 45, 0_2)_2]_s$ CFRP laminates ($R = +0.1$) (Cyclic stress levels; % of failure stress: ----- 67, —77, – – – 93).

is that while the random distributions of broken fibres in the 0° plies (evidence of which is provided by edge replication) must affect both the notched and un-notched strengths equally, the resin or interface cracks in the 45° plies appear to facilitate the propagation of a precut notch, either by providing additional easy crack paths or by effectively "sharpening" the tip of the precut notch (as in the case of weak grain boundaries in a notched ceramic sample). It is interesting to note that the inverse effect occurs when a pre-notched sample is subjected to fatigue cycling: it is commonly observed that the fatigue stress concentration factor, K_f, falls during cycling as a result of localized deformation in the notch tip region or in the vicinity of a hole [24, 25].

A "map" of the effects observed in these experiments is given in Fig. 20, which is a plot of all measured K_Q and σ_f data pairs together with the line representing Equation 2. It can be seen that the effects of damage are not as simple as might have been expected. First, the net reduction in K_Q/σ_f for the CFRP as a result of cycling, over the range of stresses and cycles used, is small (about 11%), although both strength and toughness are affected by the fatigue damage. Second, transverse compression of CFRP results in a reduction in σ_f without any significant change in K_Q, with the result that the K_Q/σ_f ratio rises. Third, transverse compression of GRP samples results in little change in σ_f, but a marked upward shift in K_Q, with an accompanying net upward shift in K_Q/σ_f. Finally, stress corrosion of the GRP results in no significant change in either K_Q or σ_f. These several trends are illustrated by the arrows in Fig. 20. In addition, but not plotted in Fig. 20, repeated impact to high cumulative levels of absorbed impact energy also result in no net change in the toughness–strength ratio of the woven-roving glass–epoxy laminate.

Transverse compression loading of the GRP laminate left no visible signs of microstructural damage, and during subsequent tensile testing the acoustic emission response of the damaged samples gave no indication of the presence of prior damage. The tensile strength of the material was not affected by the compression, but the notched strength was increased, as shown in Fig. 20. Since there was no visible fibre fracture or resin cracking, the source of the increase in toughness must be related to the plastic deformation of the resin, possibly with some local rearrangement of the fibres. By contrast, the CFRP did sustain substantial damage, with visible evidence of fibre fractures, resin deformation, and resin cracking. The higher the level of such prior damage, the greater the level of acoustic emission activity during subsequent tensile testing, in accordance with expectation. At very high levels of damage (91%), the strength of the laminate is reduced to 0.72 GPa. The ratio of the damaged

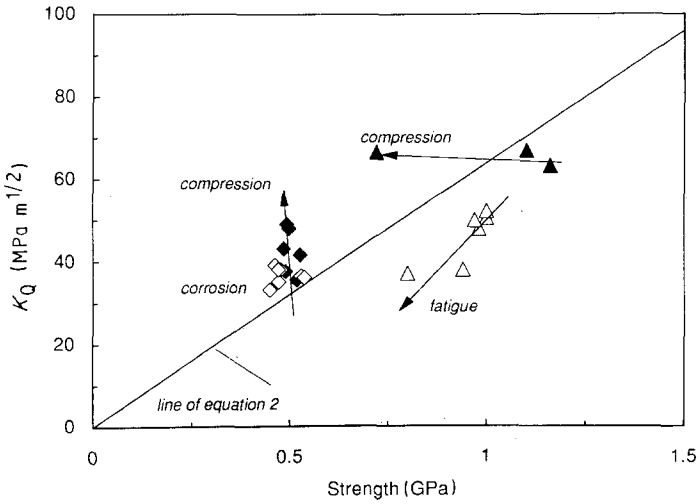

Figure 20 Changes in the K_Q/σ_f ratio as a consequence of prior damage induced in various ways (△CFRP, ◇ GRP).

strength to the undamaged strength is thus 0.64, which is close to the value of the ratio σ_N/σ_f for a notched composite, as discussed earlier. The level of fibre damage associated with this high degree of compression is likely to be responsible for this reduction in strength although, as shown by the AE results in Fig. 9, the overall spectrum of microstructural damage mechanisms is not altered by the damage. Similarly, the failure of the notched samples was apparently not changed by the transverse compression damage, implying that the notch sensitivity of the damaged material is actually reduced by the damage.

Stress corrosion of a GRP composite results principally in stress corrosion fractures of the reinforcing fibres and although there are also likely to be some resin cracks associated with these fibre fractures, the extent of this will not approach that of the large-scale, off-axis ply cracking found in the fatigued or compressively loaded CFRP composites. The damage induced by stress corrosion is likely to be similar to that which would be sustained during the ordinary loading of an undamaged sample to failure, and we would not, therefore, expect any marked change in the tensile strength, which is precisely what was observed. In this case, too, the un-notched strength is also unaffected by the corrosion and yet of all the forms of damage induced in these experiments, it is the corrosion that has brought about the most clear cut and progressive changes in the AE behaviour (Fig. 17). We conclude, therefore, that the acoustic emission effects observed both during the initial induction of the damage and during subsequent tensile testing were associated only with damage in the outer 45° plies, and that this does not markedly affect the mechanical properties of the GRP, unlike the through thickness damage induced in the CFRP by transverse compression and fatigue.

The notched strength of the CFRP was drastically reduced by repeated impact, whereas that of the woven-roving GRP remained unaffected by both the slow compression and the impact conditions. The difference is probably due to a combination of effects. The properties of the epoxy resin matrices are rate-dependent, and they would, therefore, appear more prone to brittle cracking under impact conditions, but the woven reinforcement in the GRP will always help to localize the effects of the impact damage [26], whereas the non-woven ply structure of the quasi-isotropic CFRP does nothing to inhibit the more widespread cracking in the 45° plies. It is generally acknowledged that localized impact on a CFRP laminate generates large areas of damage within the volume of the material [27]. The result is that the damage tolerance of the GRP is equally good under slow loading and impact conditions, whereas that of the CFRP is good under slow compression, despite the visible evidence of damage shown in Fig. 6, but poor under impact conditions.

Thus, it appears that under various circumstances, the effects of microstructural damage may result in independent changes in the notched and un-notched strengths of a composite. However, there appears not to be a simple pattern of changes. The toughness to strength ratio, K_Q/σ_f, may rise or fall, depending on the material and the damaging conditions, as shown in Fig. 20. However, the results for all of the tests presented here still fall within the 90% confidence limits for the relationship of Equation 2 identified in the survey of Harris *et al.* [8].

These new results, therefore, answer no questions about the significance of the 1 mm "critical defect size". The only significant observed change in the ratio K_Q/σ_f, by a factor less than two for a very heavy compression load exerted over an area of some 400 mm^2, suggests that the size of the damage zone itself bears no relation to the fracture mechanism.

5. Conclusions

The conclusions are as follows.

(1) Tensile fatigue cycling of a $[(\pm 45, 0_2)_2]_s$ CFRP laminate results in fibre and matrix damage that lead to reductions in both the notched and un-notched strength and an overall reduction of some 11% in the ratio K_Q/σ_f.

(2) Both glass and carbon fibre reinforced epoxy laminates of $[(\pm 45, 0_2)_2]_s$ construction are tolerant of damage induced by high levels of transverse compression, despite the fact that the CFRP showed evidence of substantial fibre, matrix and interface damage. Severe local damage in these laminates slightly increased the apparent toughness of the GRP and reduced that of the CFRP, with only very slight or no changes in the tensile strength. The net effect of these changes was, nevertheless, to increase the K_Q/σ_f ratio slightly for both materials.

(4) Stress corrosion of a GRP laminate brought about no significant changes in either the strength or the toughness.

(5) Woven-roving and CSM glass–resin composites appear highly tolerant of repeated impact damage, despite extensive visible signs of damage (stress whitening). The small reductions in the strength and toughness of the WR glass–epoxy composite were such as to give no net change in the K_Q/σ_f ratio. The CFRP laminate, on the other hand was much less tolerant of impact damage.

Acknowledgement

A. S. Chen wishes to acknowledge the financial support of the British Council for the period of his research programme at the University of Bath.

References

1. J. M. WHITNEY and R. J. NUISMER, *J. Compos. Mater.* **8** (1974) 253–265.
2. R. J. NUISMER and J. M. WHITNEY, ASTM STP 593, (American Society for Materials and Testing, Philadelphia, 1975) pp. 117–138.
3. R. B. PIPES, R. C. WETHEROLD and J. W. GILLESPIE, *J. Compos. Mater.* **13** (1979) 148–160.
4. M. E. WADDOUPS, J. R. EISENMANN and B. E. KAMINSKI, *ibid.* **5** (1971) 446–454.
5. G. DOREY, "Damage Tolerance in Advanced Composite Materials," RAE (Farnborough), Technical Report TR 77172, Ministry of Defence (Procurement Executive) (1977).

6. G. DOREY, "Relationships Between Impact Resistance and Fracture Toughness in Advanced Composite Materials," AGARD (NATO) Lecture Series number CP-288 (1980).
7. R. C. WETHEROLD and M. A. MAHMOUD, *Mater. Sci. Eng.* **79** (1986) 55–65.
8. B. HARRIS, S. E. DOREY and R. G. COOKE, *Comp. Sci. Technol.* **31** (1988) 121–141.
9. F. J. BELZUNCE, A. GUTIÉRREZ and J. VIÑA, Proceedings of the Sixth Meeting of El Grupo Español de Fractura, Sevilla, Spain, March 1989, edited by J. Dominguez Abascal, J. Garcia-Lomas Jung and A. Navarro Robles (El Grupo Español de Fractura, Sevilla, 1989) pp. 211–216.
10. C. ZWEBEN, *J. Mech. Phys. Solids*, **19** (1971) 103–116.
11. *Idem., J. Compos. Mater.* **3** (1969) 713.
12. J. O. OUTWATER and M. C. MURPHY, Proceedings of the 24th Annual Technical Meeting of the Reinforced Plastics/ Composites Institute of SPI, (SPI, New York, 1969) Paper no. 11-C.
13. S. S. WANG, J. F. MANDELL and F. J. McGARRY, ASTM STP 593 (American Society for Testing and Materials, Philadelphia, 1975) pp. 36–85.
14. F. J. GUILD, F. J. ACKERMAN, M. G. PHILLIPS and B. HARRIS, Proceedings of the First International Symposium on Acoustic Emission from Reinforced Composites, San Francisco (SPI, New York, 1983), Paper A-4, 1–14.
15. F. J. GUILD, M. G. PHILLIPS and B. HARRIS, *J. Mater. Sci. Lett.* **4** (1985) 1375–1378.
16. J. MORTON and E. W. GOODWIN, *Compos. Structures* **13** (1989) 1–19.
17. T. M. TAN and C. T. SUN, *J. Appl. Mech.* **107** (1985) 6–12, also reprinted in *Trans ASME*, **52** (1985) 6–12.
18. J. R. WILLIS, *J. Mech. Phys. Solids*, **14** (1966) 163–176.
19. F. J. GUILD, M. G. PHILLIPS and B. HARRIS, *NDT International*, **13** (1980) 209–218.
20. J. BECHT, H. J. SCHWALB and J. EISENBLATTER, *Composites* **7** (1976) 245.
21. T. J. FOWLER, "Acoustic Emission Testing of Fibre Reinforced Plastics," ASCE Convention, San Francisco, USA, Preprint 3092 (1977).
22. G. DOREY, P. SIGÉTY, K. STELLBRINK and W. G. J. 't HART, "Impact Damage Tolerance of Carbon Fibre and Hybrid Laminates (GARTEUR TP-037), RAE (Farnborough), Technical Report TR 87057, Ministry of Defence (Procurement Executive) (1987).
23. P. C. PARIS and G. C. SIH, ASTM STP 381 (American Society for Testing and Materials, Philadelphia, 1965) pp. 30–81.
24. R. PRABHAKARAN and M. K. SRIDAR, Proceedings of the 30th Annual Technical Meeting of the Reinforced Plastics/ Composites Institute of SPI (SPI, New York, 1975) Paper no. 9-D.
25. B. HARRIS, A. O. ANKARA, D. CAWTHORNE and S. M. T. BYE, *Composites* **8** (1977) 185–189.
26. B. HARRIS, *Met. Sci.* **14** (1980) 351–362.
27. W. J. CANTWELL and J. MORTON, *Compos. Structures* **13** (1989) 101–114.

Received 1 December 1989
and accepted 9 January 1990